

Article

# Shoal-to-Strata Ratio Technique and Its Use in Describing Carbonate Rock Sedimentary Facies in the Eastern Sichuan Basin

Xiuquan Hu <sup>1,2</sup> , Hong Liu <sup>1,\*</sup>, Xiucheng Tan <sup>1</sup>, Chenjing Xiao <sup>2</sup>, Qian Tan <sup>2</sup>, Jianghan Li <sup>2</sup> and Chi Yi <sup>2</sup>

<sup>1</sup> School of Earth Science and Technology, Southwest Petroleum University, Chengdu 610091, China; huxiuquan15@cdut.edu.cn (X.H.); tanxiucheng70@163.com (X.T.)

<sup>2</sup> College of Energy, Chengdu University of Technology, Chengdu 610059, China; chenjing\_xiao@163.com (C.X.); tanqian19@cdut.edu.cn (Q.T.); lijianghanhan@163.com (J.L.); cdutyichi@163.com (C.Y.)

\* Correspondence: nd123@163.com

**Abstract:** The requirements for the accurate characterization of shoal sediments have increased in view of the fact that strata are eroded due to uplift and it is difficult to calculate the real thickness of granular shoal. To solve this problem, with the shoal-to-strata ratio, the type and distribution range of carbonate rock shoal facies are described, and the characterization of sedimentary facies is subsequently presented. Taking the P<sub>2</sub>m<sup>2</sup>a in Eastern Sichuan as an example, the following conclusions were obtained. (1) The primary rock types of the shoal facies of the P<sub>2</sub>m<sup>2</sup>a are bioclastic limestone and micrite limestone. The logging facies of platform margin shoals, intra-platform high-energy shoals, intra-platform low-energy shoals, and sloping low-energy shoals are large funnel-type, small funnel-type, box-type, and finger-like, respectively. The platform margin shoals and intra-platform high-energy shoals are imbricate seismic facies, and the intra-platform low-energy shoals and sloping low-energy shoals are S-type progradation seismic facies and oblique progradation. (2) The shoal-to-strata ratio of platform margin shoals is the highest, followed by intra-platform high-energy shoals, intra-platform low-energy shoals, and sloping low-energy shoals. (3) Shoal facies deposits have a certain controlling effect on gas production, and platform margin shoals have greater exploration potential. (4) This example shows that in the areas where carbonate rock strata are eroded, compared with the method of characterizing the sedimentary facies of carbonate rock using the shoal thickness, the shoal-to-strata ratios are more accurate. (5) The planar distribution diagram of the shoal-to-strata ratio can be used as a supporting map for compiling sedimentary facies maps. This method is worth applying in related research fields.

**Keywords:** shoal-to-strata ratio; carbonate rock shoal facies; Eastern Sichuan area; carbonate rock P<sub>2</sub>m<sup>2</sup>a; platform margin



**Citation:** Hu, X.; Liu, H.; Tan, X.; Xiao, C.; Tan, Q.; Li, J.; Yi, C. Shoal-to-Strata Ratio Technique and Its Use in Describing Carbonate Rock Sedimentary Facies in the Eastern Sichuan Basin. *J. Mar. Sci. Eng.* **2022**, *10*, 825. <https://doi.org/10.3390/jmse10060825>

Received: 24 April 2022

Accepted: 14 June 2022

Published: 16 June 2022

**Publisher's Note:** MDPI stays neutral with regard to jurisdictional claims in published maps and institutional affiliations.



**Copyright:** © 2022 by the authors. Licensee MDPI, Basel, Switzerland. This article is an open access article distributed under the terms and conditions of the Creative Commons Attribution (CC BY) license (<https://creativecommons.org/licenses/by/4.0/>).

## 1. Introduction

As development and research related to the oil and gas sector continuously increase, it is necessary to carry out sedimentary facies analysis to identify favorable reservoir facies belts. The study of sedimentary facies and sub-facies, especially microfacies, is vital for the development of subtle oil and gas reservoirs [1,2]. In recent years, it has been found that a large amount of oil and gas is stored in the reservoirs of shoal facies [3–5], indicating that favorable shoal facies are important for the formation of oil and gas reservoirs [3,6–13]. An important factor restricting the progress of oil and gas exploration is the poor understanding of the distribution regularity of shoal facies [14,15]. Many researchers have conducted extensive research on shoals, including the study of sedimentary environments [16], controlling factors [17,18], and types and depositional patterns of shoals [19]. The results from previous studies have shown that shoal facies can be formed in sedimentary environments of carbonate platforms, platform edges, gentle slopes, and tidal flats [16,20–22]. The

quality of carbonate shoal facies reservoirs is controlled by sedimentary microfacies and micro-paleo-geomorphic fluctuations.

In this study, we focused on granular shoals. Previous studies have shown that changes in the thickness of granular rocks contribute to changes in micro-topography during the depositional period. These changes control the likelihood of shoal facies developing. Therefore, tracking changes in the thickness of granular rocks is the basis for the study of sedimentary microfacies and the restoration of microtopography [23,24]. Presently, the criteria for the traditional division of carbonate shoal facies are primarily based on the cumulative thickness of the granular rocks. Taking each well as a control point, together with statistical analysis of the cumulative thickness of granular rocks in the layer section of an individual well, the distribution of granular shoal thickness can be plotted. Shoal sedimentary facies were divided according to the thickness of the granular shoal. Combined with the development zone of shoal sedimentary facies, the planar distribution of the sedimentary facies was classified. For example, Chen (2014) divided the shoal facies development zone of the Maokou Formation in Eastern Sichuan based on the thickness of the granular shoals [25]. The greater the thickness of the granular shoal, the more developed the shoal facies and the higher the depositional energy. Accordingly, the planar distribution of the sedimentary facies in the Maokou Formation was clearly observed. However, the existing study methods of shoal facies sedimentation rely heavily on the cumulative thickness of granular rocks, without considering the influence of unconformities on the thickness of granular shoals in some areas. The Maokou Formation in the Eastern Sichuan Basin has been exposed for 1–3 Ma [26] owing to differential uplift during the DongWu Movement. The strata experienced varying degrees of denudation, up to  $P_2m^2a$  in some areas. However, the strata thickness of layers in the same section varies widely across different areas, which may cause a significant change in the thickness of the granular shoal. This is not a result of differences in sedimentary microfacies but rather from the influence of exposure and denudation. Therefore, when dividing sedimentary facies according to the thickness of the granular shoal without considering the thickness difference caused by denudation, the difference in sedimentary regularity cannot be truly reflected. This oversight may contribute to the failure of oil and gas exploration. To eliminate the influence of the difference in the thickness of the granular shoal caused by exposure and denudation of the strata, the distribution range of carbonate rock shoal facies in  $P_2m^2a$  was studied using the shoals-to-strata ratio technique, and the sedimentary facies in the strata were characterized accurately. In this study, we focused our work on the Eastern Sichuan Basin in China.

## 2. Geological Background

The Eastern Sichuan region is under the jurisdiction of the Chongqing–Fuling Line and includes counties such as Kaijiang, Wanzhou, Dazhu, Dianjiang, Fengdu, Yubei, and Fuling in Chongqing (Figure 1). It is located in the southern Sichuan Basin, among Mounts Huaying, Qiyao, and Daba. There are numerous ejective folds trending northeast–southwest in Eastern Sichuan from west to east. This abnormally developed fault belt includes Tongluo Gorge, Mingyue Gorge, and Huangnitang [25,27–29].

In early Permian times, the Sichuan Basin experienced extensive uplift and denudation, and marine transgression occurred, forming high paleogeography in the west and low paleogeography in the east. At the same time, the Liangshan, Qixia, Maokou, and Longtan Formation/Wujiaping Formations were deposited successively in the eastern Sichuan Basin. During the early depositional period of the Maokou Formation, tectonic extension intensified, and the Sichuan Basin experienced the largest transgression event throughout South China in the Permian. The sedimentary environment in Eastern Sichuan was mainly a deep-water, mud-rich, open-sea environment. In the middle depositional period of the Maokou Formation, sea levels continued to decrease, and the development area of shoals increased. Under the joint control of basement faults and the extensional structural environment [30,31], tectonic extension activity was further intensified. The craton intra-

platform extensional trough developed in northeastern Sichuan, and platform marginal deposits developed along the extensional trough. During the late depositional period of the Maokou Formation, due to the DongWu Movement, the entire Eastern Sichuan area was uplifted, and the Maokou Formation was severely eroded. The uneroded area is dominated by open platform facies with abundant shoals.

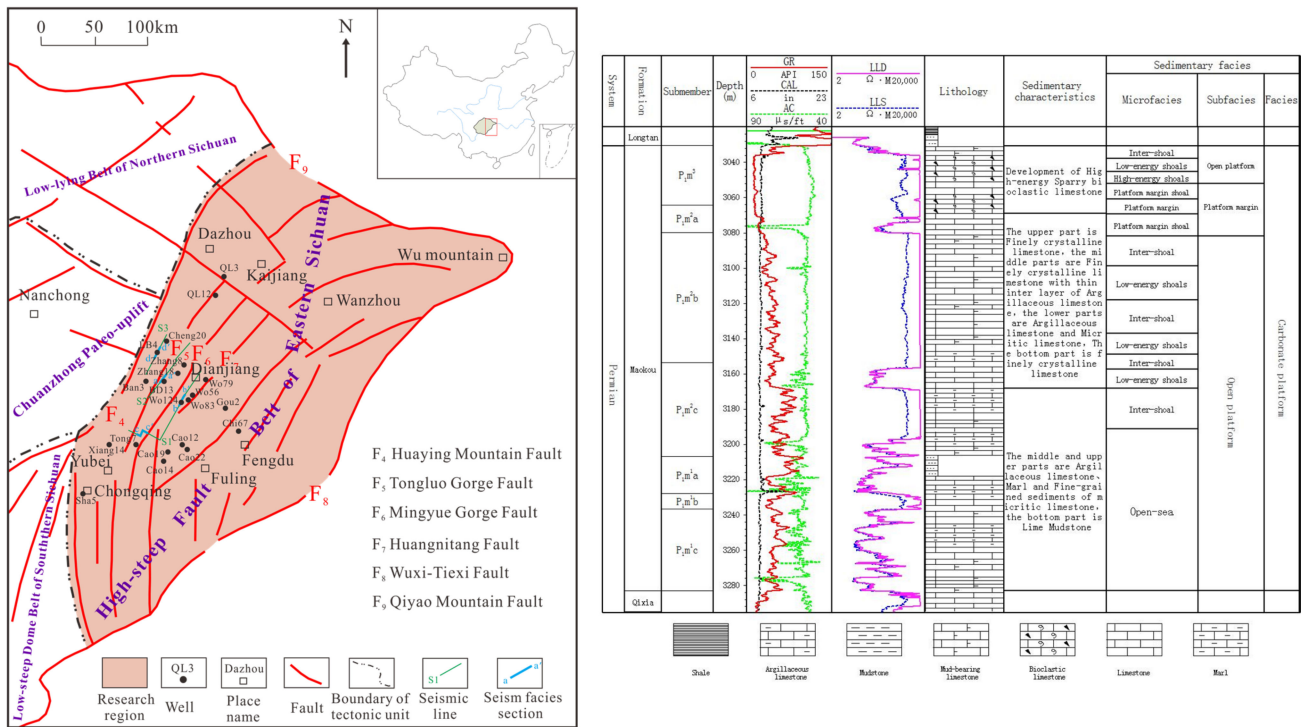


Figure 1. Geographical location map of study area showing relevant fault lines and wells (modified from [21]), and comprehensive histogram of Well Ban3.

According to the characteristics of lithological change, the Maokou Formation in Eastern Sichuan can be divided into four sections from bottom to top: Mao 1, Mao 2, Mao 3, and Mao 4. The second section of the Maokou Formation, Mao 2 (also referred to as P<sub>2m</sub><sup>2</sup>), can be further divided into subsections a, b, and c. The Maokou Formation underwent varying degrees of denudation owing to the DongWu movement. The thickness of the residual stratum was 50–210 m, with significant variation. Many eyelid and eyeball limestones developed in the Mao 1 section, and bioclastic limestone developed in the Mao 2 section. In P<sub>2m</sub><sup>2a</sup> and P<sub>2m</sub><sup>2b</sup>, gray to dark gray medium-thick micritic bioclastic limestone developed, which was well stratified. In the P<sub>2m</sub><sup>2c</sup> subsection, mainly bioclastic micritic limestone and argillaceous limestone developed, which are locally characterized by eyeball eyelid structures. In the Mao 3 section, gray to dark gray medium-thick layered micritic bioclastic limestone and bioclastic limestone developed, with many karst caves as well (Figure 1). The Mao 4 section is severely eroded, and can only be observed locally in the south, with the development of a weathering crust on the top.

### 3. The Technical Workflow for the Method of the Shoal-to-Strata Ratio

The workflow for the characterization of carbonate rock sedimentary facies using the shoal-to-strata ratio as a technical method is as follows (Figure 2):

- (1) Conduct a statistical study on the cumulative thickness of the granular limestone and the thickness of the strata in the studied layer section.

$$h = \sum_{i=1}^n h_i$$

where  $h$  is the cumulative thickness of the granular limestone,  $n$  is the number of granular limestone layers, and  $h_i$  is the thickness of the  $i$ th layer of granular limestone.

$$H = D_1 - D_2$$

where  $H$  is the thickness of the strata,  $D_1$  is the bottom depth of the studied layer section, and  $D_2$  is the top depth of the studied layer section.

- (2) Calculate the ratio of the cumulative thickness of the granular limestone to the thickness of the strata in the layer section under study, that is, the shoal-to-strata ratio.

$$R = \frac{h}{H}$$

where  $R$  is the shoal-to-strata ratio,  $H$  is the thickness of the strata, and  $h$  is the cumulative thickness of granular limestone.

- (3) Compared with the single-well facies division, good correlation, and reservoir physical properties for determining the minimum empirical threshold of shoal facies and the range value of various types of shoal facies, the values above indicate shoal facies deposits.
- (4) The shoal-to-ground ratio plane was compiled according to the minimum empirical threshold and range of the various types of shoal facies.
- (5) Based on the plane view of the shoal-to-strata ratio combined with analytical methods (rock thin section identification, cathodoluminescence, etc.), the planar distribution of sedimentary facies is plotted, and the characterization of sedimentary facies of carbonate rock is described.

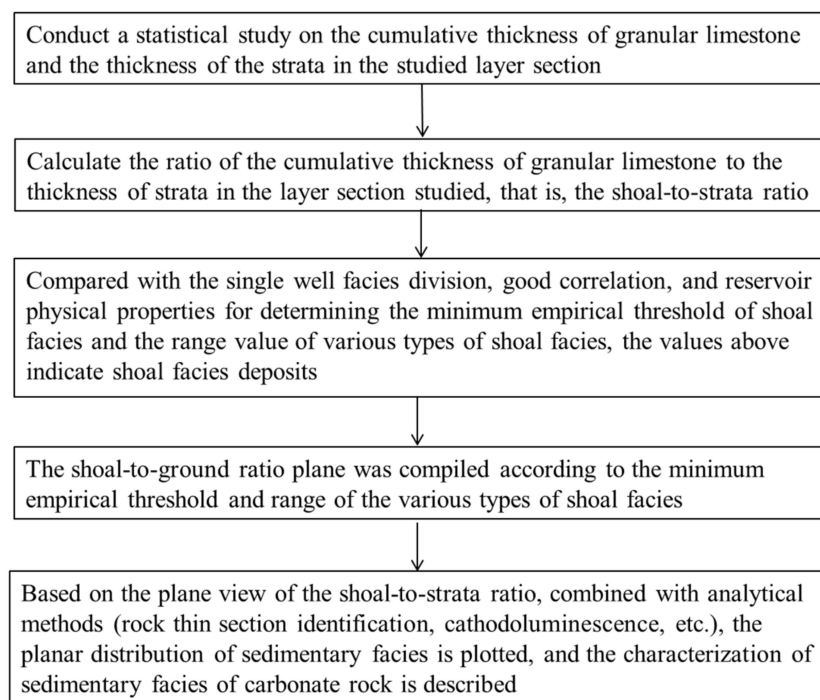


**Figure 2.** Flowchart of characterization of sedimentary facies of carbonate rocks using shoal-to-strata ratio.

## 4. Application Example

### 4.1. Markers for Shoal Identification

Field observations, drilling data, and core thin section observation results were combined with a comprehensive analysis of logging curves. In addition, the carbonate sedimentary facies division scheme based on the method by Wilson [32] suggests that  $P_2m^2a$  in Eastern Sichuan is mainly composed of carbonate rock platform deposits, with the development of four sub-facies, including open platform, platform margin, slope, and basin. These sub-facies can further be divided into eight types of microfacies: intra-platform high-energy shoal, intra-platform low-energy shoal, inter-shoal, open-sea, platform margin shoal, sloping low-energy shoal, sloping mud, and ocean trough. By analyzing the petrological and logging characteristics of different types of shoals in  $P_2m^2a$ , the markers for the identification of shoals were summarized.

#### 4.1.1. Petrological Markers

According to the classification scheme of carbonate rock proposed by Dunham [33], the primary rock types of shoal facies of the  $P_2m^2a$  in the Eastern Sichuan area are granular limestone and micrite limestone, with the observation of cores from limited coring wells and thin section identification. The granular type includes bioclastic and algal debris and one or several combinations. Bioclastic grains are primarily in the study area, with cement dominated by sparry calcite and microcrystalline calcite.

The platform margin shoal facies are distributed locally in  $P_2m^2a$ , Eastern Sichuan. It is mainly characterized by a thick, layered-massive, stable distribution at the macroscopic level. The lithology is mainly sparry bioclastic limestone, sparry oolitic limestone, and micritic granular limestone, with the development of flint nodule limestone locally. The platform margin shoal facies differ from other shoal facies in terms of the high content of bioclastic sparry. Dolomitization is high; dolomite is only occasionally found in the platform margin shoal of  $P_2m^2a$  in the study area. Moreover, the degree of dolomitization of granular limestone is high. Bioclastics are mainly brachiopods, algae, and other paleontologies. Locally, wave-resistant corals are visible, indicating a high-energy wave-resistant environment with deposits of the platform margin (Figure 3). The intra-platform high-energy shoal is distributed locally in  $P_2m^2a$  in Eastern Sichuan, and it is mainly in a stable and thick-layered massive distribution macroscopically. The lithology is mainly sparry bioclastic limestone and micritic bioclastic limestone locally, with the development of flint nodule limestone in the area. Bioclastics have a high degree of crystallization; some of the bioclastic body cavities are filled with sparry calcite, and some bioclastics are in an oriented arrangement (Figure 4). Intra-platform low-energy shoals are widely distributed and dominated by micritic bioclastic limestone and micritic limestone. The bioclastic grains are mainly brachiopods, bivalves, gastropods, foraminifera, and mixed stacking of a small amount of algae. The bioclastics were broken, and micrite occurred at the crust biogenic shell edge. There are mainly two burial forms: chaotic melt and stratiform stacking (Figure 5). The sloping low-energy shoal is distributed locally and is thin- to medium-layered. The lithology is mainly micritic limestone with less development of micritic bioclastic limestone. Generally, the bioclastic content is low, and the bioclastic grains are mainly composed of shells.

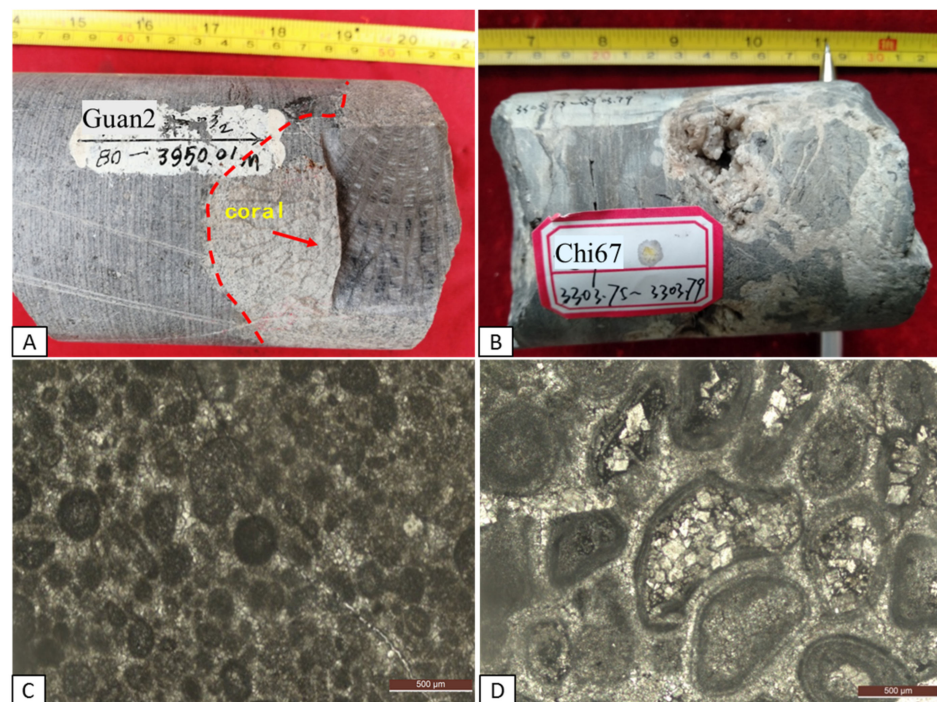


**Figure 3.** Petrological characteristics of platform margin shoal in  $P_2m^2a$ , Eastern Sichuan. (A) Bioclastic limestone with the development of coral in well Gou2. (B) Dolomite in well Chi67; the pores are filled with saddle dolomite. (C) Sparry oolitic and arenaceous limestone in well Wo83. (D) Sparry oolitic limestone in well Wo83, in which the oolitic particles are dolomitized.

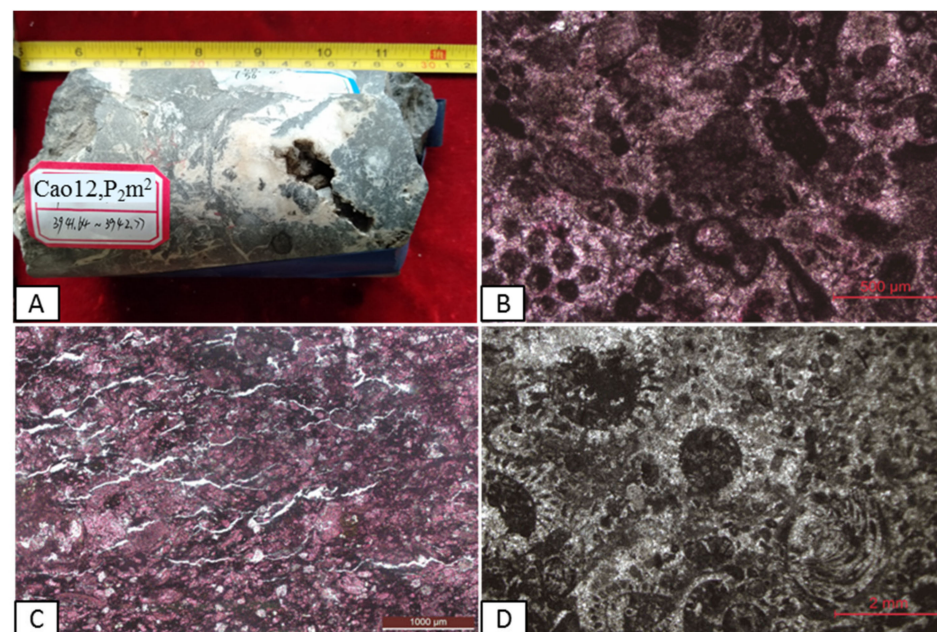


**Figure 4.** Petrological characteristics of intra-platform high-energy shoal in  $P_2m^2a$ , Eastern Sichuan. (A) Sparry arenaceous and bioclastic limestone with unfilled dissolved pores in well Cao12. (B) Sparry bioclastic and arenaceous limestone in well Xiang14. (C) Dolomitic limestone with a high degree of biological sparry in well Cao12. (D) Sparry algal clast limestone in well Cao22.

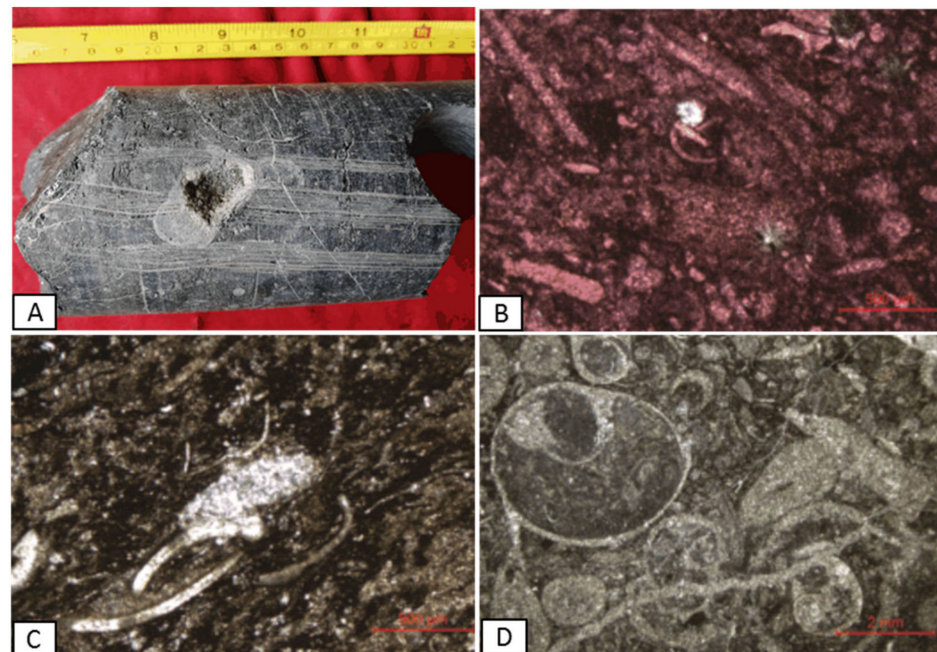


**Figure 5.** Petrological characteristics of intra-platform low-energy shoal in  $P_2m^2a$ , Eastern Sichuan. (A) Micritic bioclastic limestone with partially filled dissolved pores in well Cao14. (B) Micritic bioclastic limestone with the development of bivalves in well Cao14. (C) Bioclastic micritic limestone with high organic matter content in well Tong7. (D) Micritic bioclastic limestone with the development of gastropods and foraminifera in well Cao22.

#### 4.1.2. Logging Facies Markers

Well logging information can reflect the various physical properties of rocks [34–36], and different logging response characteristics indicate lithological changes in different sedimentary environments [25,37–39]. Among the many logging curves, the natural gamma curve reflects changes in the sedimentary environment [40,41]. Through a comparative analysis between core observations and thin section identification with the study results of natural gamma curves, it was found that the GR value of shoal facies sedimentary rocks was low. The GR value of the platform margin shoal facies was generally less than 27 API. The overall shape of the GR curve is a large funnel-type. The morphology of the GR curve shape shows abrupt contact at the bottom, and the GR value is low at the top, showing a small tooth shape (Figure 6a). The logging face of a platform marginal shoal indicates the strong hydrodynamic conditions of the sedimentary environments. The GR value of the intra-platform high-energy shoal was generally less than 30 API. The overall shape of the GR curve is a small funnel-type. The morphology of the GR curve shape shows abrupt contact at the bottom, and the GR value is low in the middle-upper part, showing a small tooth shape (Figure 6b). Compared with the platform margin beach, its bottom mutation degree is relatively small. The logging face of intra-platform high-energy shoal indicates shallow and strong hydrodynamic conditions in the sedimentary environment. The GR value of the low-energy shoal on the platform was generally less than 36 API. The GR curve is micro-serrated box-shaped (Figure 6c), indicating that the sedimentary environments were characterized by shallow water bodies and strong hydrodynamic conditions. The GR value of the sloping low-energy shoal was generally less than 42 API, showing a finger-like curve and indicating a low-energy deep-water sedimentary environment (Figure 6d).

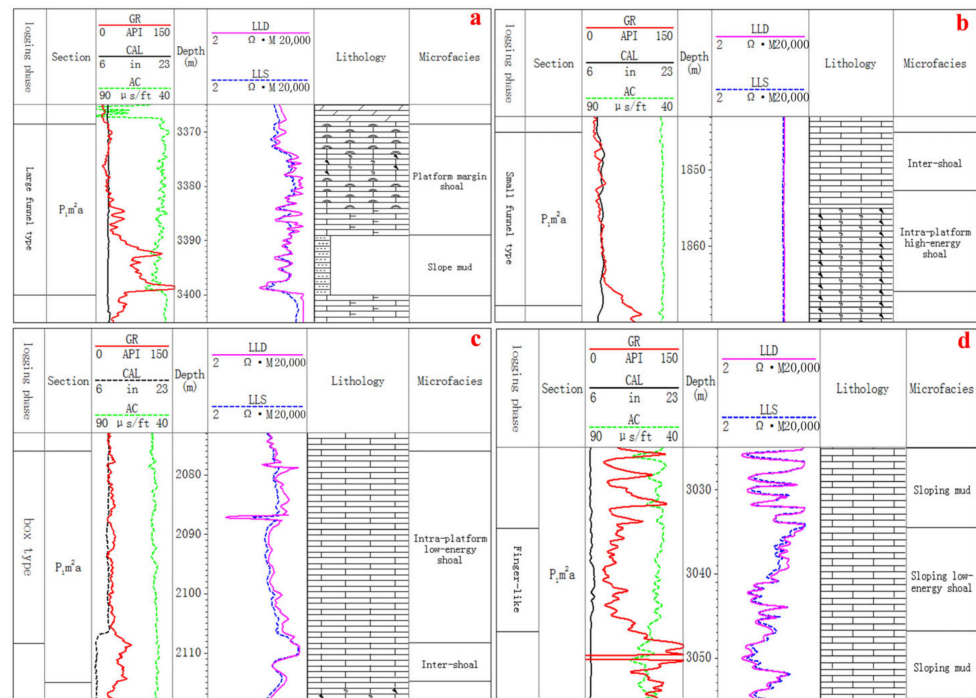


**Figure 6.** Logging facies pattern diagrams of different shoal facies deposits in Eastern Sichuan. (a) Large funnel-type, platform margin shoal in well Chi12. (b) Small funnel-type, high-energy shoal in well Xiang14. (c) Box-type, low-energy shoal in well Cao14. (d) Finger-like, sloping low-energy shoal in well LB4.

#### 4.1.3. Seismic Facies Markers

A seismic facies unit can be defined as a sedimentary unit, which is different from adjacent units in its seismic characteristics. Parameters that should be taken into consideration in the seismic facies analysis are as follows: reflection amplitude, dominant reflection frequency, reflection polarity, interval velocity, reflection continuity, reflection configuration, abundance of reflections, geometry of seismic facies unit, and relationship with other units [42,43]. Seismic facies analyses can be used to understand underground lithology, sedimentary environment, and the development of favorable reservoirs [44–46]. Different sedimentary facies often behave differently in seismic facies, particularly in high-energy turbulent sedimentary environments that show obvious abnormal seismic facies. The study area is located in the Eastern Sichuan tectonic belt, where high and steep faults are developed, the overall quality of 2D seismic data is poor, the signal-to-noise ratio is low, and the seismic imaging quality is poor. When the seismic attribute analysis was carried out, the seismic attribute effect at the location of the fault zone was not obvious, and the distribution range of the fault zone in the study area was very large. The abnormal seismic facies in the study area were identified as pro-gradational.

Using drilling calibration, the platform-margin shoal and high-energy shoal in the platform on the seismic section are mainly characterized by imbricate seismic facies (Figures 7 and 8). The specific reflection characteristics are as follows: there are several groups of slightly inclined, parallel, and poor continuity reflection waves between the two parallel reflection layers, which have an imbricate arrangement, no top or bottom layers, and only foreset bedding, indicating strong energy. The study area is an imbricated structure with a slow dip angle; the local phase axis becomes longer, and the dip angle becomes larger, which is mostly a medium-strong variable amplitude. The low-energy shoal in the platform is mainly characterized by S-type progradation seismic facies (Figure 9). The specific reflection characteristics are as follows: the reflection wave on the seismic profile is S-shaped. The single reflection layer begins to

form a horizontal reflection layer, inclines downward, unfolds gently, and oversteps downward to the bottom boundary. Generally, it has complete topset, foreset, and bottomset beds, indicating that the energy is general and the amplitude is strong. The sloping low-energy beach shows oblique progradation seismic facies in the seismic profile, and the specific reflection characteristics are as follows: the lower part of the progradation layer gradually intersects with the bottom in a tangent shape, with a progradation layer, bottom layer, and no top layer (Figure 10). The indicating energy is stronger than the S-type progradation and weaker than the imbricate progradation, and the amplitude is mostly strong and medium-strong.

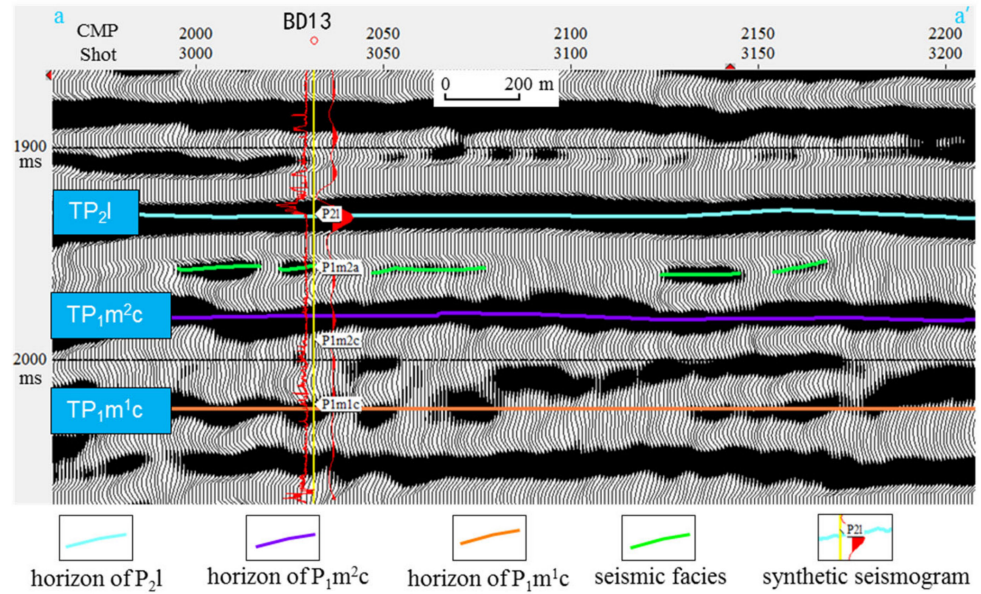


Figure 7. Seismic facies of imbricate progradation (seismic line through Well BD13).

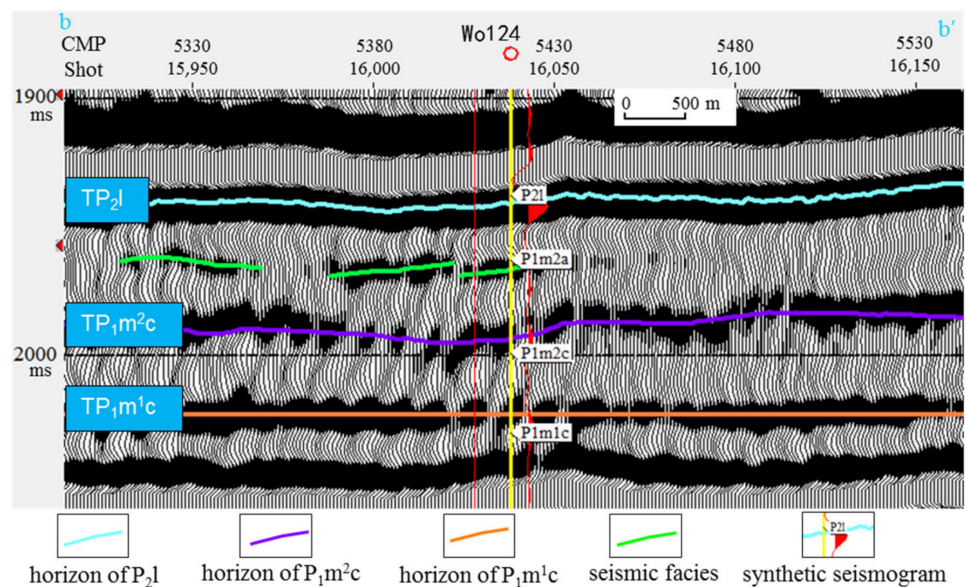


Figure 8. Seismic facies of imbricate progradation (seismic line through Well Wo124).

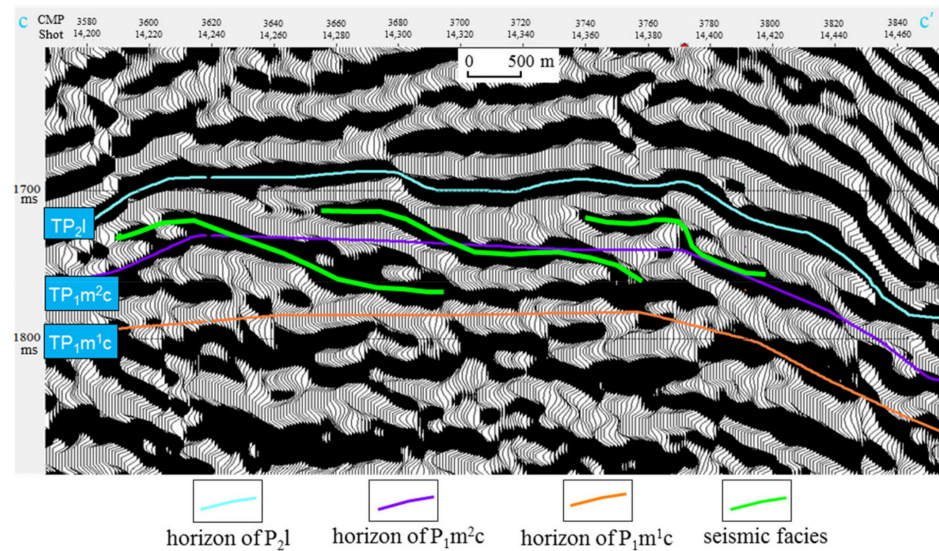


Figure 9. Seismic facies of S-type progradation.

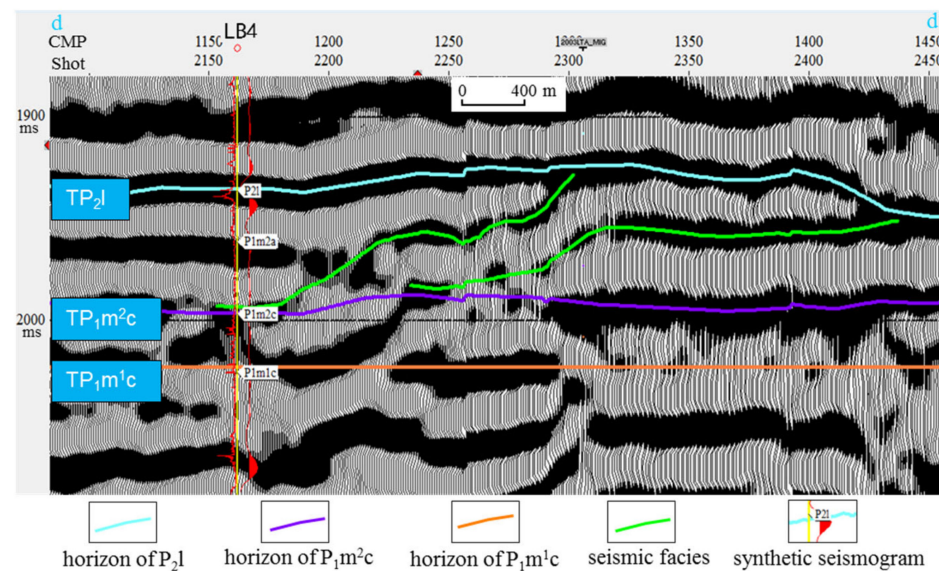


Figure 10. Seismic facies of oblique progradation (seismic line through Well LB4).

#### 4.2. Joint Well Correlation Analysis of Sedimentary Facies

A joint well correlation analysis of sedimentary facies was conducted in the study area to study the sedimentary evolution of shoal facies in  $P_2m^2a$  in Eastern Sichuan. Based on the comprehensive correlation analysis of sedimentary facies of the Maokou Formation from the joint well section, we found that the sedimentary facies belts changed remarkably in the vertical direction. Open platforms mainly developed during the depositional period of the Mao 1 section to the Mao 2b subsection. Open platforms, platform margins, slopes, and low-energy shoals within the platforms were relatively developed in the Mao 2a subsection owing to sedimentary differentiation. Platform margin shoals, intra-platform low-energy shoals, and sloping low-energy shoals were also developed. Open platforms mainly developed during the depositional period of the Mao 3 section, (Figures 11 and 12). Horizontally, the sedimentary facies were in the sequence of open platform, platform, platform margin, slope, and basin during the deposition of  $P_2m^2a$  from southwest to northeast. Intra-platform low-energy shoals were widely developed in the Yubei–Changshou area of Chongqing, with platform marginal shoals sparsely distributed in the Fengdu–Linshui area and sloping low-energy shoals distributed in Dianjiang–Dazhu.

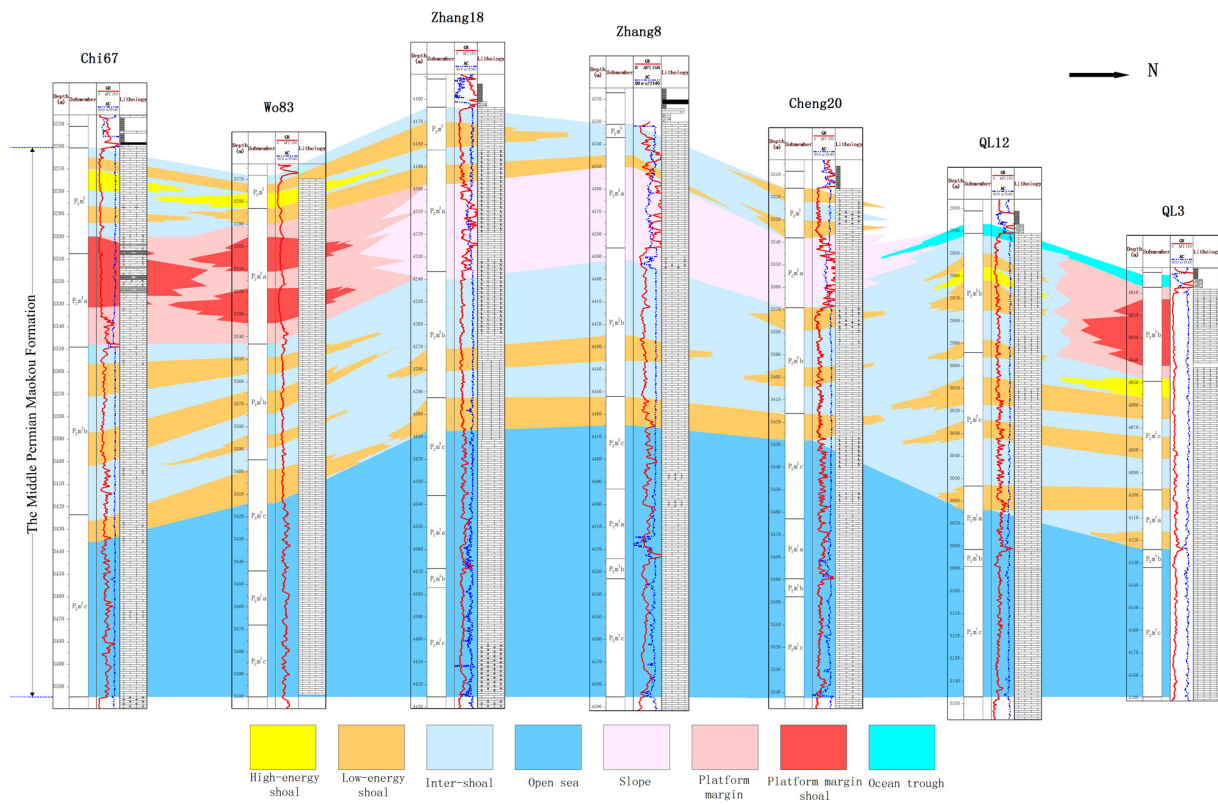


Figure 11. Sedimentary correlation section of wells Sha5-Xiang14-Ban3-Zhang18-Wo79-Wo83-Chi67 in Eastern Sichuan.

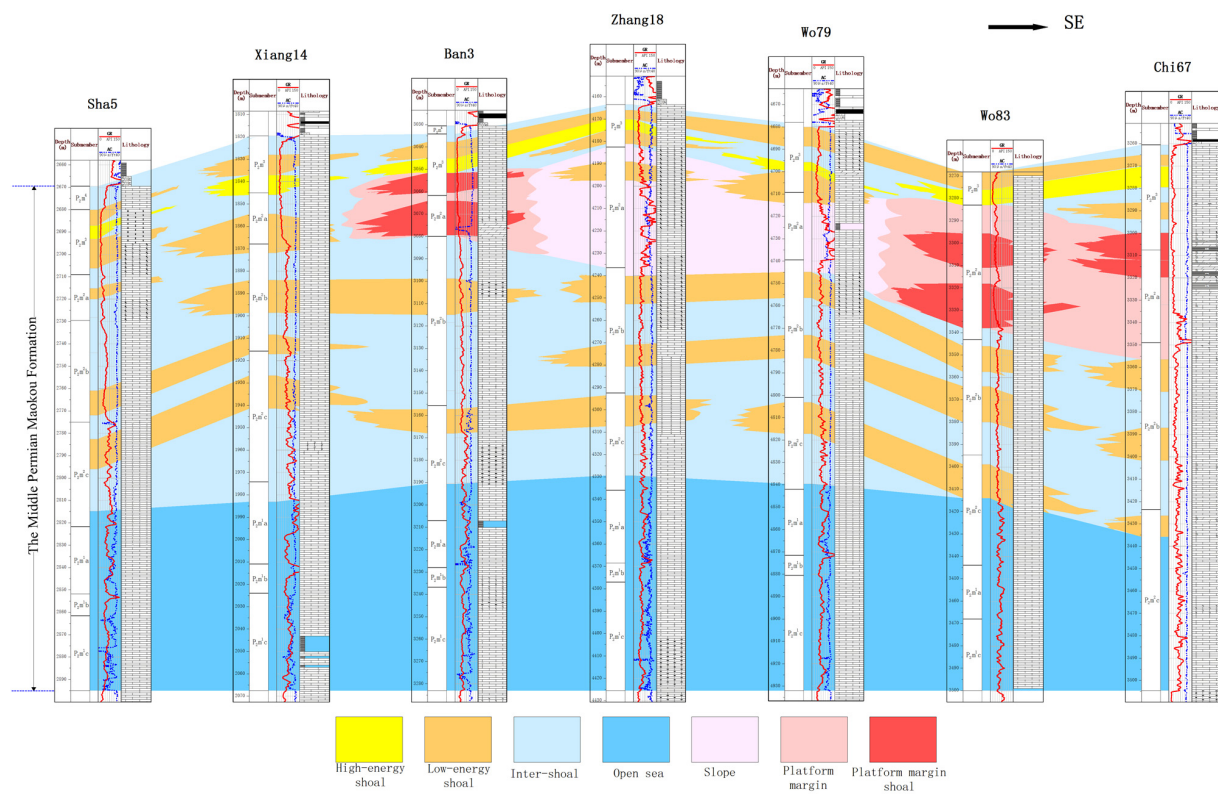


Figure 12. Sedimentary correlation section of wells Chi67-Wo83-Zhang18-Zhang8-Cheng20-QL12-QL3 in Eastern Sichuan.

#### 4.3. Statistical Analysis of Shoal-to-Strata Ratio

This is example 1 of an equation:

The quality of carbonate rock shoal facies is strictly controlled by sedimentary microfacies and micro-paleo-geomorphic undulation, whereas the thickness variation of granular rocks can roughly characterize the change in micro-topography during the depositional period. However, the DongWu movement led to the uplift of the Maokou Formation in Eastern Sichuan, resulting in the denudation of the stratum. In the most severely denudated area, denudation can reach  $P_2m^2a$ , resulting in a large variation in the thickness of the granular shoal, which does not truly reflect the difference in the sedimentation regularity. Therefore, in this study, we proposed to use the shoal-to-strata ratio to analyze the development of granular shoals in the  $P_2m^2a$ .

A detailed analysis of sedimentary facies was carried out on 64 key wells in the study area. In addition, the cumulative thickness of the granular limestone, the stratigraphic thickness of  $P_2m^2a$ , and the shoal-to-strata ratio were calculated (Table 1). In the comparison of the ratio with individual-well sedimentary facies, it was found that the wells with a ratio of shoals to the whole strata greater than 0.3 have highly developed reservoirs, the cementation of grainstone with a ratio between 0.3 and 0.5 is micrite, and the grain type is bioclast. The cements of grainstone with a ratio between 0.5 and 0.8 are sparry, the grain types are algal clasts, oolitic clasts, and bioclasts, and wave-resistant paleontology is occasionally seen. Therefore, the shoal-to-strata ratio was greater than or equal to 0.3 for shoal facies, 0.3–0.5 for intra-platform low-energy shoals or sloping low-energy shoals, 0.5–0.6 for intra-platform high-energy shoals, and 0.6–0.8 for platform margin shoals. The larger the ratio, the more developed the shoal facies deposits and the higher the depositional energy. There were 34 sets of data for  $P_2m^2a$ , with a shoal-to-strata ratio greater than or equal to 0.3 in the Eastern Sichuan area. A planar graph of the shoal-to-strata ratio was compiled with an interval of 0.1 (Figure 13). The shoal deposits of the  $P_2m^2a$  are mainly distributed in the central and southern parts of the study area, with the shoal-to-strata ratios ranging from 0.3 to 0.5, locally reaching 0.7–0.8.

**Table 1.** Statistical data of the shoal-to-strata ratio in the  $P_2m^2a$ , Eastern Sichuan.

Well	Stratum Thickness/m	Cumulative Thickness of Granular Limestone/m	Shoal-to-Strata Ratio	Well	Stratum Thickness/m	Cumulative Thickness of Granular Limestone/m	Shoal-to-Strata Ratio
BX1	19	12	0.6	QL11	3.6	0.5	0.1
Ban2	28.2	22	0.8	QL12	4	0	0
Ban3	9.1	7.1	0.8	QL13	10.2	5.3	0.5
BD13	52.5	36	0.7	QL22	4.5	0	0
BD9	51	14	0.3	QL28	4.2	0	0
Cao12	46.5	22	0.5	QL3	3.6	0	0
Cao15	47.9	18	0.4	QL48	15	0	0
Cao20	44.5	18	0.4	QL5	1.8	0	0
Cheng20	31	7	0.2	QL50	3.1	0	0
Cheng23	14.5	1	0.1	QL54	4.3	1	0.2
Chi10	22.5	1	0	QL9	7	0	0
Chi12	31.5	23	0.7	Sha5	20.5	8	0.4
Chi19	25.4	11	0.4	SH2	35.5	11	0.3
Chi20	32.6	14	0.4	Tan1	23.2	6	0.3
Chi32	48.5	28	0.6	TD11	3.3	0	0
Chi6	83.5	3	0	TD30	55	5	0.1
DS1	28	11	0.4	TX2	43.5	15	0.3
Feng11	3.5	0.5	0.1	TX3	3	0	0

Table 1. Cont.

Well	Stratum Thickness/m	Cumulative Thickness of Granular Limestone/m	Shoal-to-Strata Ratio	Well	Stratum Thickness/m	Cumulative Thickness of Granular Limestone/m	Shoal-to-Strata Ratio
Feng7	3	0	0	TX4	41	5	0.1
Feng9	4.2	0.5	0.1	Wo124	32	24	0.8
FE4	29	15	0.5	Wo44	35	11	0.3
Gou2	43	28.3	0.7	Wo77	59	35	0.6
Guan2	1.9	0	0	Wo79	53.5	23	0.4
LD1	36	9	0.3	Wo83	60.1	34	0.6
Liang1	37	16	0.4	Wo92	43.2	26.5	0.6
Liang3	32	2.3	0.1	WT1	6	1.6	0.3
Liang9	36	10	0.3	Xiang14	22.9	12	0.5
LB3	48.5	10	0.2	Yue4	37	22	0.6
LB4	58	16	0.3	YA21	5.4	1.2	0.2
MN1	11	0	0	YA3	3	0.5	0.2
MX6	7.7	0	0	Zhang17	32.3	12	0.4
QL013-H1	4.2	0.8	0.2	Zhang8	49	6	0.1

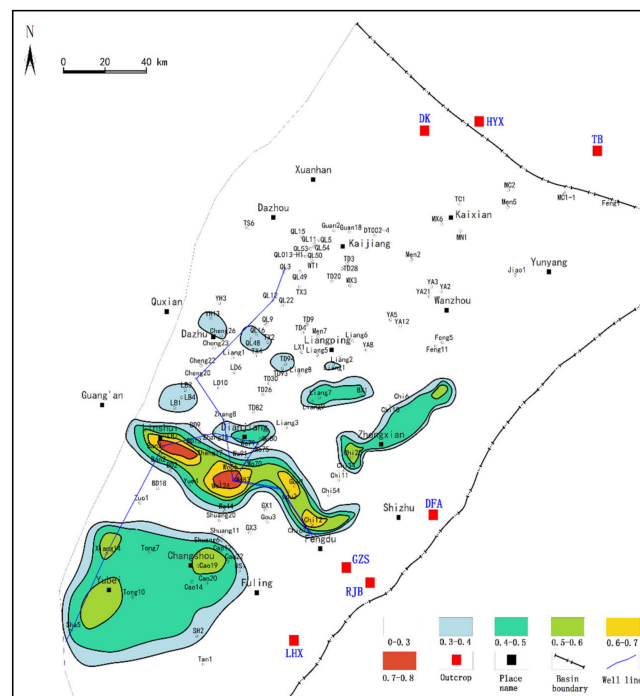


Figure 13. Planar distribution of shoal-to-strata ratio in the P<sub>2</sub>m<sub>2</sub>a.

## 5. Discussion

### 5.1. Method Applicability

The shoal-to-strata ratio of sedimentary facies is mainly used to classify sedimentary facies by avoiding the influence of the granular rock thickness difference caused by denudation. This method has minimal applicability and is time-consuming and labor-intensive. When the strata are not denudated, the thickness of the granular rock can be used to classify sedimentary facies. Hence, the shoal-to-strata ratio of land need not be used to classify the sedimentary facies. The thickness and corresponding ratio of the stratum need not be calculated, which is time-saving and results in the rapid description of carbonate sedimentary facies. However, when the strata are denuded, it is unreasonable to use the thickness of rock to classify the sedimentary facies. The influence of the denudation and the thickness of the rock particles cannot fully reflect the differences in the sedimentary

microfacies. Therefore, the shoal-to-strata ratio should be used to classify the sedimentary facies. Although this method is time-consuming and cost-intensive, the accuracy of the description of sedimentary facies has greatly improved. Therefore, the method to classify sedimentary facies must be chosen based on the geological background to achieve better results.

### 5.2. Planar Distribution Characteristics of Sedimentary Facies

Combining regional tectonic evolution and sedimentary background with the petrological markers, logging facies markers, and inter-well correlation of sedimentary facies, a planar distribution map of sedimentary facies of  $P_2m^2a$  was plotted (Figure 14). The plot was based on the planar diagram of the shoal thickness/stratigraphic thickness ratio. Combined with analysis and testing methods, the carbonate rock sedimentary facies were characterized. During the depositional period of  $P_2m^2a$ , the sedimentary facies belts spread from southwest to northeast in the Eastern Sichuan area in the sequence of open platform, platform, margin, slope, and basin. The paleogeographical high open platform is characterized by a relatively shallow water body and strong hydrodynamic conditions. In high-energy environments, sediments are influenced by hydrodynamic conditions, resulting in relative enrichment of granular sediments. The low-energy and high-energy shoals within the platform are high-quality reservoirs that are worth exploring within the platform. The low-energy shoals are mainly distributed in the area with a shoal-to-strata ratio of 0.3–0.5, and the scale of the low-energy shoal body was large. The high-energy shoals in the platform were mainly distributed in the area with a ratio of 0.5–0.6, and the scale of the high-energy shoal body was moderate. The platform margin of  $P_2m^2a$  was approximately distributed in a striped pattern, striking in the EW direction. The platform margin shoal, with high sedimentary energy, was sporadically developed in the interior, and the ratio was approximately 0.6–0.8. The sloping low-energy shoal was sporadically distributed in the sloping sub-facies in the geomorphological bottom, and the ratio was approximately 0.3–0.5. There was a good relationship between the shoal deposits and the shoal-to-strata ratio value and distribution area. The greater the shoal-to-strata ratio, the stronger the hydrodynamic force and the greater the exploration potential.

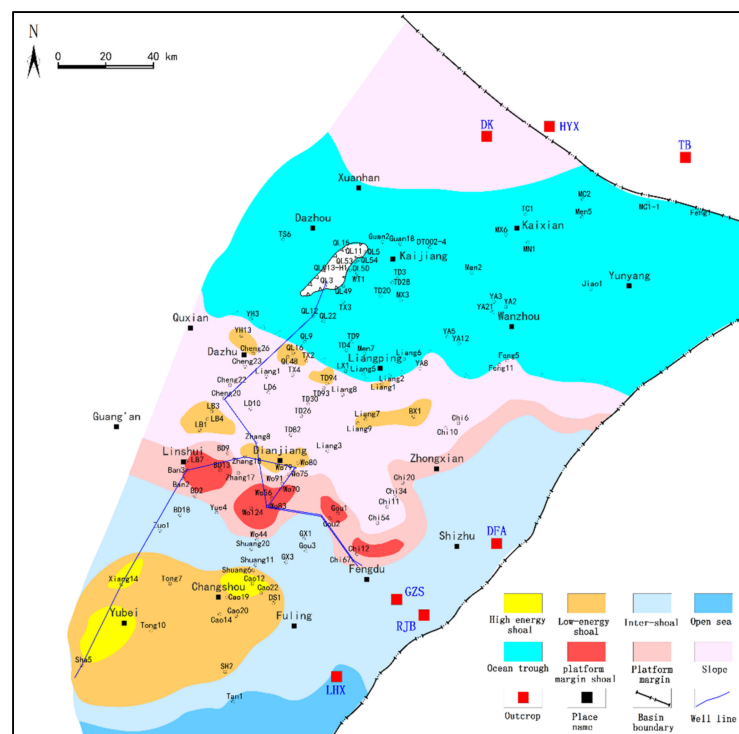
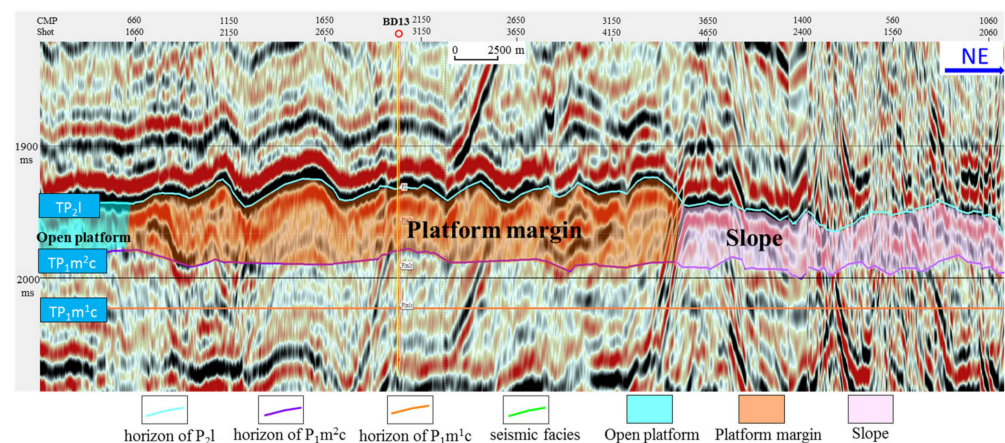


Figure 14. Planar distribution of sedimentary facies in the  $P_2m^2a$ .

### 5.3. Discovery of Platform Margin in Eastern Sichuan

Before 2015, it was mainly believed that the overall sedimentary environment of the Maokou Formation in the Sichuan Basin was characterized by an open platform or ramp platform. In the late stage, the formation was affected by tectonic uplift and suffered weathering and denudation, and a karst fracture-cavity reservoir was developed. Since then, some scholars considered that the platform margin shoal of the late Maokou Formation might have developed in northern Sichuan based on the drilling seismic data of the whole basin [47]. In 2018, Well Yuanba 7 in northern Sichuan encountered the platform margin shoal reservoir of the Maokou Formation and obtained high-yield industrial gas flow. Its daily production is higher than that of the intraplatform beach reservoir, which confirmed the existence of the platform margin of the Maokou Formation in the Sichuan Basin for the first time and has broad exploration prospects. Therefore, we must change our concepts and re-learn the sedimentary facies types and distribution of the Maokou Formation in Eastern Sichuan according to the developing platform margin in late Maokou. This earlier study proposed the view that the platform margin was developed in the vicinity of the Linshui–Fengdu–Zhongxian area in  $P_2m^2a$  in Eastern Sichuan, and that the platform margin shoal is an important reservoir. Important evidence shows that the main rock type of the shoal facies in  $P_2m^2a$  is sparry bioclastic limestone, which has a high bioclastic sparry and dolomitization content. Bioclastics are mainly brachiopods, algae, and other paleontologies. Locally, wave-resistant corals are visible, indicating a high-energy wave-resistant environment. It is particularly worth mentioning that another important piece of evidence for the development of platform margin facies in the Maokou Formation in Eastern Sichuan is that there were obvious differences in the stratigraphic thickness on the seismic profile. The thickness of the platform margin was significantly greater than that of the platform and slope, and the external morphology was slightly hilly (Figure 15).



**Figure 15.** Platform margin deposition of Maokou Formation in Eastern Sichuan.

### 5.4. Significance to Exploration of Oil and Gas

Sedimentary facies are the material basis for the formation of reservoirs, and sedimentary environments control the physical properties and scale of the reservoir [48–50]. The quality of reservoirs deposited in different sedimentary environments varies significantly [51–53]. Many studies have shown that platform margin shoal, intra-platform shoal, and other shoal facies are important zones for oil and gas exploration in carbonate rock reservoirs. Oil and gas exploration is particularly concentrated in platform margin belts [54]. In Well Yuanba 7 in northeastern Sichuan, platform margin shoal facies of the Maokou Formation were encountered, obtaining high-yield industrial gas flow, with daily gas production of  $105.9 \times 10^8 \text{ m}^3$  [47]. These results confirm that the carbonate rock platform margin shoal facies of the Maokou Formation have significant exploration potential.

Analyses were conducted on the gas testing results of the different shoal facies in  $P_2m^2a$  in Eastern Sichuan (Table 2). The wells with oil and gas deposits were mainly

distributed in the platform margin shoal facies. When conducting production tests in Well Wo67, the production capacity of the platform marginal shoal in P<sub>2</sub>m<sup>2</sup>a was  $50 \times 10^4$  m<sup>3</sup>/d. The daily gas production of Well Wo77, which had the lowest gas flow among the platform marginal shoal facies, was also  $3.18 \times 10^4$  m<sup>3</sup>/d. Oil and gas flows were also obtained in drilling wells that encountered an intra-platform high-energy shoal in P<sub>2</sub>m<sup>2</sup>a, with gas production of  $5.74 \times 10^4$  m<sup>3</sup>/d. The results show that the shoal has a certain controlling effect on oil and gas production, and the platform margin shoal has greater exploration potential than a high-energy shoal. The platform margin shoal facies of the Maokou Formation in the study area are favorable for the development of large and medium-sized gas fields.

**Table 2.** Corresponding relationship between gas test results and sedimentary facies.

Well	Test Results ( $\times 10^4$ m <sup>3</sup> /d)	Practical Production Layer	Sedimentary Facies
Wo67	50	Mao 2a	Platform margin shoal
Wo83	25.53	Mao 2a	Platform margin shoal
Wo93	8.38	Mao 2a	Platform margin shoal
BD11	3.89	Mao 2a	Platform margin shoal
Wo77	3.18	Mao 2a	Platform margin shoal
Xiang3	5.74	Mao 2a	High-energy shoal

## 6. Conclusions

- (1) In areas where carbonate rock strata are eroded, the shoal-to-strata ratio can accurately reflect the types and distribution of granular shoals compared with the use of shoal thickness to classify the sedimentary facies of carbonate rocks. By comparing the ratio values, the types of shoal bodies can be determined more accurately, and the development of granular shoals in the studied layer section can be analyzed.
- (2) A new view of the platform margin development in the Maokou Formation in Eastern Sichuan is proposed, and the platform margin shoal is an important reservoir. In the Eastern Sichuan area, the distribution of sedimentary facies belts of P<sub>2</sub>m<sup>2</sup>a is in the sequence of open platform, platform margin, slope, and basin, from southwest to northeast. Intra-platform low-energy shoals and sloping low-energy shoals are mainly distributed in areas with a shoal-to-strata ratio of 0.3–0.5, intra-platform high-energy shoals are distributed in areas with a ratio of 0.5–0.6, and platform margin shoals are mainly distributed in areas with a ratio of 0.6–0.8. The gas production test results show that deposits of shoal facies control oil and gas production, and platform margin shoals have greater exploration potential than intra-platform high-energy shoals.
- (3) The planar distribution diagram of the shoal-to-strata ratio can be used as an important supporting map for compiling sedimentary facies. It can help researchers quickly and accurately determine sedimentary environments and make plans for future exploration. The application results are positive, indicating that this method is worth popularizing and applying in related research fields.

**Author Contributions:** Conceptualization, X.H. and H.L.; Formal analysis, H.L., X.T. and Q.T.; Funding acquisition, X.H.; Investigation, C.X., J.L. and C.Y.; Methodology, X.H. and H.L.; Writing—original draft, X.H. and C.X.; Writing—review and editing, X.T. and Q.T. All authors have read and agreed to the published version of the manuscript.

**Funding:** This study was supported by the National Natural Science Foundation of China (Grant No. 42172175).

**Institutional Review Board Statement:** Not applicable.

**Informed Consent Statement:** Not applicable.

**Data Availability Statement:** The data are contained within the article.

**Acknowledgments:** The authors of this research thank all of the researchers who contributed to the research process during our study.

**Conflicts of Interest:** The authors declare no conflict of interest.

## References

- Chen, G.H.; Wang, Z.W.; Li, D.Y.; Zhang, J.Y.; Xu, S.S. Automatic discriminant sedimentary microfacies by means of multivariate statistics analysis. *Pet. Geophys.* **1997**, *36*, 71–76.
- Deng, R.; Meng, F.S. On Logging Curves Fine Delamination to Identify Sedimentary Microfacies. *Well Logging Technol.* **2010**, *34*, 554–558. [[CrossRef](#)]
- Ruf, M.; Aigne, T. Facies and poroperm characteristics of a carbonate shoal (Muschelkalk South German Basin): A reservoir analogue investigation. *J. Pet. Geol.* **2004**, *27*, 215–239. [[CrossRef](#)]
- Bádenas, B.; Aurell, M. Facies models of a shallow-water carbonate ramp based on distribution of non-skeletal grains (Kimmeridgian, Spain). *Facies* **2010**, *56*, 89–110. [[CrossRef](#)]
- Kargarpour, M.A. Carbonate reservoir characterization: An integrated approach. *J. Pet. Explor. Prod. Technol.* **2020**, *10*, 2655–2667. [[CrossRef](#)]
- Mancini, E.A. *Integrated Geologic-Engineering Model for Reef and Carbonate Shoal Reservoirs Associated with Paleohighs: Upper Jurassic Smackover Formation, Northeastern Gulf of Mexico*; University of Alabama: Tuscaloosa, AL, USA, 2003. [[CrossRef](#)]
- Petrovic, A.; Aigner, T. Are shoal reservoirs discrete bodies: A coquina shoal outcrop analogue from the mid Triassic upper muschelkalk, SW Germany. *J. Pet. Geol.* **2017**, *40*, 249–275. [[CrossRef](#)]
- Yu, Y.; Sun, L.; Song, X.; Guo, R.; Gao, X.; Lin, M.; Yi, L.; Han, H.; Li, F.; Liu, H. Sedimentary diagenesis of rudist shoal and its control on reservoirs: A case study of Cretaceous Mishrif Formation, H Oilfield, Iraq. *Pet. Explor. Dev.* **2018**, *45*, 1075–1087. [[CrossRef](#)]
- Idan, R.M.; Salih, A.L.; Al-Khazraji, O.N.; Khudhair, M.H. Depositional Environments, Facies Distribution, and Porosity Analysis of Yamama Formation in Majnoon Oilfield. Sequence Stratigraphic Approach. *Iraqi Geol. J.* **2020**, *53*, 38–52. [[CrossRef](#)]
- Abbas, L.K.; Mahdi, T.A. Reservoir Modeling of Mishrif Formation in Majnoon Oil Field, Southern Iraq. *Iraqi Geol. J.* **2020**, *53*, 89–101. [[CrossRef](#)]
- Wang, H.; Zhou, Q.M.; Zhou, W.; Zhang, Y.D.; He, J.H. Carbonate Platform Reef-Shoal Reservoir Architecture Study and Characteristic Evaluation: A Case of S Field in Turkmenistan. *Energies* **2022**, *15*, 226. [[CrossRef](#)]
- Lv, H.T.; Ding, W.L.; Yun, L.; Liu, Q. Middle-lower Ordovician carbonate reservoir karst-fracture characteristics in the southwest region of Tahe Oilfield. *Geoscience* **2009**, *24*, 699–708.
- Duan, J.B.; Ji, C.H.; Zhang, X.F. Development mechanism of reef reservoir of the Permian and Triassic strata in northern Sichuan Basin, China. *J. Chengdu Univ. Technol. Nat. Sci. Ed.* **2016**, *43*, 423–430.
- Li, R.B.; Fan, T.L.; Gao, Z.Q.; Hu, X.L. Characteristics and influencing factors of reservoirs in the Ordovician Yinshan Formation of the ka1 three dimensional seismic area within Katake uplift, Tarim basin. *Geol. China* **2011**, *38*, 1016–1025.
- Liu, H. The Development and Distribution Characteristics of Bank of Reservoir Changxing Formation in Yuanba Area. Master's Thesis, Chengdu University of Technology, Chengdu, China, 2012.
- Tucker, M.E.; Wright, V.P. *Carbonate Sedimentology*; Blackwell Publishing: London, UK, 1990.
- Gao, Z.Q.; Fan, T.L.; Li, Y.; Liu, W.H.; Chen, Y.L. Study on Eustatic Sea-Level Change Rule in Cambrian-Ordovician in Tarim Basin. *J. Jilin Univ. Earth Sci. Ed.* **2006**, *36*, 50–552. [[CrossRef](#)]
- Tan, X.C. Geological Model of Complicated Carbonate Reservoir with Multi-Cycle: Exemplified by Jia2 Gas Pool of Moxi Structure of Middle Sichuan. Ph.D. Thesis, Chengdu University of Technology, Chengdu, China, 2007.
- Zhao, J.X.; Li, F.J.; Liu, Q.; Jiang, B. Analysis on Permian Sedimentary Facies and Its Lithofacies Palaeogeographic Evolution, Northeast Sichuan Basin. *Nat. Gas Sci.* **2008**, *19*, 444–451.
- Flügel, E. *Microfacies Analysis of Limestones*; Springer: Berlin/Heidelberg, Germany, 1982; pp. 1–633.
- Balthaser, L.H. Microfacies Analysis of Limestones. *Mar. Geol.* **1983**, *52*, 303–304. [[CrossRef](#)]
- Flügel, E. *Microfacies of Carbonate Rocks*; Springer: Berlin/Heidelberg, Germany, 2010.
- Liu, H.; Tian, X.C.; Zhou, Y.; Li, J.L.; Lin, J.P.; Li, Q.; Feng, Y. Logging facies of granular carbonate rock and its implication on reservoir evaluation. *Nat. Gas Geosci.* **2007**, *18*, 527–530.
- Tan, X.C.; Nie, Y.; Liu, H.; Zhou, Y.; Li, L.; Zhao, L.Z.; Zhang, B.J.; Feng, Y. Research on the Method of Recovering of Microtopography of Epeiric Carbonate Platform in Depositional Stage: A case study from the layer A of Jia22 Member in Moxi Gas Field, Sichuan Basin. *Acta Sedimentol. Sin.* **2011**, *29*, 486–494. [[CrossRef](#)]
- Chen, Y.Q. Distribution Regularity of Grain Beach of Middle Permian Maokou Formation in Eastern Sichuan and Its Control on Weathering Crust Karst. Master's Thesis, Southwest Petroleum University, Chengdu, China, 2014.
- He, B.; Xu, Y.G.; Wang, Y.M.; Xiao, L. Nature of the Dongwu Movement and Its Temporal and Spatial Evolution. *Geosci.-J. China Univ. Geosci.* **2005**, *30*, 89–96.
- Luo, B.; Wang, W.F.; Chen, Y.Q.; Xiao, D.; Cheng, Y.; Li, S.; Xu, F.B.; Tan, X.C. Sedimentary Characteristics of Middle Permian Maokou Algal Framework Reef Rock in the East of Sichuan Basin. *Mar. Orig. Pet. Geol.* **2015**, *20*, 53–61.

28. Wang, X.Z.; Tang, Y.; Yu, T.; Chen, J.Z. Restoration of karst landform of Maokou Formation in eastern Sichuan and its geological significance. *China Pet. Chem. Stand. Qual.* **2019**, *39*, 191–192.
29. Chen, H. The Restoration of Sedimentary Paleogeomorphology of Maokou Formation of Lower Permian in East Sichuan and Karst Reservoir Research. Master's Thesis, Chengdu University of Technology, Chengdu, China, 2020.
30. Wang, H.; Shen, H.; Huang, D.; Shi, X.W.; Li, Y.; Yuan, X.L.; Yang, Y.R. Origin and distribution of hydrothermal dolomites of the Middle Permian in the Sichuan Basin. *Nat. Gas Ind.* **2014**, *34*, 25–32.
31. Wang, L.J.; Yang, C.; Wang, Q.B.; Jia, G.G. Hydrothermal dolomite reservoir prediction for Maokou formation in Fuling area, Sichuan basin. *Comput. Tech. Geophys. Geochem. Explor.* **2018**, *40*, 298–305.
32. Wilson, J.L. *Carbonate Facies in Geologic History*; Springer: Berlin/Heidelberg, Germany, 1975.
33. Dunham, R.J. Classification of carbonate rocks according to their depositional texture. In *Classification of Carbonate Rocks—A Symposium*; Ham, W.E., Ed.; Memoir 1; American Association of Petroleum Geologists: Tulsa, OK, USA, 1962; pp. 108–121.
34. Pirson, S.J. *Geologic Well Logs Analysis*; Gulf Publishing Corporation: Houston, TX, USA, 1978.
35. Serr, O. *Fundamental of Well-Log Interpretation 2: The Interpretation of Logging Data*; Elsevier Science Publishers BV: Amsterdam, The Netherlands, 1986; pp. 180–185.
36. Klett, M.; Eichhorst, F.; Schäfer, A. Facies interpretation from well logs applied to the Tertiary Lower Rhine Basin fill. *Neth. J. Geosci.* **2002**, *81*, 167–176. [[CrossRef](#)]
37. Serra, O. *Sedimentary Environment from Wire Line Logs*; Services Techniques Schlumberger: Houston, TX, USA, 1985.
38. Adeel, N.; Shabeer, A.A.; Sarfraz, H.S. Sedimentary facies interpretation of Gamma Ray (GR) log as basic well logs in Central and Lower Indus Basin of Pakistan. *Geod. Geodyn.* **2016**, *7*, 432–443. [[CrossRef](#)]
39. Fan, H.; Shi, J.Y.; Fan, T.L.; Gao, Z.; Zhang, T.H.; Li, B. Sedimentary microfacies analysis of carbonate formation based on FMI and conventional logs: A case study from the ordovician in the Tahe Oilfield, Tarim Basin, China. *J. Pet. Sci. Eng.* **2021**, *203*, 108603. [[CrossRef](#)]
40. Huang, L.J. *Radioactive Logging Principles*; Petroleum Industry: Beijing, China, 1985.
41. Asubiojo, T.M. Facies Architecture Analysis for Paleo-environment Evaluation in “Tom” Oil Field, Eastern Niger Delta, Nigeria. *J. Appl. Sci. Environ. Manag.* **2020**, *24*, 213–221. [[CrossRef](#)]
42. Roksandić, M.M. Seismic facies analysis concepts. *Geophys. Prospect.* **1978**, *26*, 383–398. [[CrossRef](#)]
43. Sheriff, R.E. *Seismic Stratigraphy*; International Human Resources Development Corp.: Boston, MA, USA, 1982; pp. 25–50.
44. Shi, Z.J.; Hu, X.Q.; Wang, C.C. Analysis of the seismic facies of Maokou Formation in the southeast of Sichuan Basin. *J. Chengdu Univ. Technol. Sci. Technol. Ed.* **2011**, *38*, 113–120.
45. Iván, D.M. A knowledge-integration framework for interpreting seismic facies. *Interpretation* **2014**, *2*, 1–9. [[CrossRef](#)]
46. Jesus, C.; Lupinacci, W.M.; Takayama, P.; Almeida, J.; Ferreira, D.J.A. An approach to reduce exploration risk using spectral decomposition, prestack inversion, and seismic facies classification. *AAPG Bull.* **2020**, *104*, 1075–1090. [[CrossRef](#)]
47. Hu, D.F. Breakthrough in natural gas exploration in the platform margin shoal at the Maokou Fm in the Yuanba area, Sichuan Basin, and its implications. *Nat. Gas Ind.* **2019**, *39*, 1–10.
48. Sallam, E.S.; Afife, M.M.; Fares, M.; Loon, A.J.V.; Ruban, D.A. Sedimentary facies and diagenesis of the Lower Miocene Rudeis Formation (southwestern offshore margin of the Gulf of Suez, Egypt) and implications for its reservoir quality. *Mar. Geol.* **2019**, *413*, 48–70. [[CrossRef](#)]
49. Leila, M.; Moscariello, A. Seismic stratigraphy and sedimentary facies analysis of the pre- and syn- Messinain salinity crisis sequences, onshore Nile Delta, Egypt: Implications for reservoir quality prediction. *Mar. Pet. Geol.* **2019**, *101*, 303–321. [[CrossRef](#)]
50. Nabawy, B.S.; Mansour, A.S.; Rashed, M.A.; Afify, W.S.M. Implementation of sedimentary facies and diagenesis on the reservoir quality of the Aquitanian-Burdigalian Rudeis Formation in the Gulf of Suez, Egypt: A comparative surface and subsurface study. *Geol. J.* **2020**, *55*, 4543–4563. [[CrossRef](#)]
51. Davies, G.R.; Smith, J.L.B. Structurally controlled hydrothermal dolomite reservoir facies: An overview. *AAPG Bull.* **2006**, *90*, 1641–1690. [[CrossRef](#)]
52. Wiczbicki, R.; Dravis, J.J.; Al-Aasm, I.S.; Harland, N. Burial dolomitization and dissolution of Upper Jurassic Abenaki platform carbonates, Deep Panuke reservoir, Nova Scotia, Canada. *AAPG Bull.* **2006**, *90*, 1843–1861. [[CrossRef](#)]
53. Luo, L. Sedimentary Facies of Qixia-Maokou Formation in Northwest Sichuan Basin. Master's Thesis, Southwest Petroleum University, Chengdu, China, 2017.
54. Zhang, J.H.; Yu, B.S.; Qi, Z.L.; Bai, Z.K.; Ruan, Z.; Li, L.R. Seismic facies and the distribution of the intraplatform shoals in the Ordovician Yingshan Formation in the Ka-1 three-dimensional seismic area, Central Tarim Basin, Xinjiang. *Sediment. Geol. Tethyan Geol.* **2016**, *36*, 104–112.